

Precision Control in Lattice Calculation of x -dependent Pion Distribution Amplitude

Jack Holligan,^{1,*} Xiangdong Ji,^{1,†} Huey-Wen Lin,^{2,3,‡} Yushan Su,^{1,§} and Rui Zhang^{1,¶}

¹*Department of Physics, University of Maryland, College Park, MD 20742, USA*

²*Department of Physics and Astronomy, Michigan State University, East Lansing, MI 48824, USA*

³*Department of Computational Mathematics, Science and Engineering,
Michigan State University, East Lansing, MI 48824, USA*

We present a new full Bjorken x -dependence analysis of the lattice quantum chromodynamics calculation for the pion distribution amplitude with controlled systematics. A leading renormalon resummation in renormalization and the perturbative matching kernel generates the power accuracy of the matching to the lightcone. Meanwhile, a small momentum log resummation is implemented for both the quark momentum xP_z and the antiquark momentum $(1-x)P_z$ inside a meson of boost momentum P_z along the z direction, allowing us to have more accurate determination of the x -dependence. Finally, we use the complementarity of the short-distance OPE and the large momentum expansion to constrain the endpoint region, thus obtaining the full-range x -dependence of the lightcone distribution amplitude.

I. INTRODUCTION

Distribution amplitudes (DAs) are important observables for both theoretical and phenomenological reasons within the realm of quantum chromodynamics (QCD). The DA of a meson describes the probability of identifying the meson in a quark-antiquark Fock state on the lightcone, carrying longitudinal momentum fractions x and $1-x$, respectively. It is also known as the leading Fock wavefunction of the meson. They are important as inputs to many exclusive processes with large momentum transfer, such as the B-meson decay, that can be factorized into the nonperturbative DA and the hard-scattering kernel [1, 2]. Although the DAs are important quantities in QCD, their properties, such as the moments, the shape and the endpoint power-law behavior are still undetermined from experiments [3–6]. A direct nonperturbative calculation of the DAs from lattice QCD is thus of great interest.

The nonperturbative physics of partons is defined on the lightcone, i.e., in the effective limit of infinite momentum. Direct calculations on the lightcone are inaccessible on the lattice due to the dependence on real time. Early calculations determined DAs by calculating their lowest moments from local twist-2 operators [7–11] or from nonlocal current-current correlators [12–15]. The local-operator calculations provide precise measurements up to the second moment of the DA [11], but the increasing noise and the nontrivial mixing in the lattice renormalization make it very difficult to access higher moments. The nonlocal-operator calculations analyze data in a certain Wilson-line-displacement z range, where the short-distance factorization is valid; this either allows us to ob-

tain the lowest few moments, or needs a model assumption to fit the x -dependence [14]. A direct x -dependence calculation is not possible in the two traditional methods.

The method of large-momentum effective theory (LaMET) [16–18] offers a different approach. We study the matrix element of equal-time, spatially separated fermion fields. After renormalization, we can extrapolate these matrix elements to infinite distance and Fourier transform to momentum space. We match the data at finite hadron-momentum to the lightcone distribution. This allows us to compute the DA over a much wider range of both distances, z , and momentum fractions, x . The first lattice calculation of the pion DA in LaMET was presented by the LP3 Collaboration in 2017 [19], where they used a boosted pion at $P_z \approx 1.3$ GeV and used a mass counterterm, δm , extracted from the Wilson-loop static potential to renormalize the matrix elements. A similar work on the kaon DA followed this work [20], studying its skewness and SU(3) symmetry, with a higher meson momentum $P_z \approx 1.7$ GeV and more precisely determined δm by fitting to Wilson loops on multiple lattice spacings. The first continuum extrapolation $a \rightarrow 0$ was presented by the MSU group with nonperturbative renormalization [21] on three lattice spacings down to $a \approx 0.06$ fm. In the latest calculation by LPC [22, 23], the lattice artifacts have been controlled well by boosting to momentum as large as $P_z \approx 2.15$ GeV, extrapolating to the continuum, and calculating at the physical pion mass $m_\pi \approx 130$ MeV.

Now, the x -dependence calculation of the DA has entered an era of high precision, where the systematic controls on the theory side become more important. One complication in the calculation of quasi-DA matrix elements comes from the linearly divergent Wilson line self-energy [24–26]. To remove the linear divergence without introducing extra nonperturbative effects, an improved renormalization in the hybrid scheme [27] with self-renormalization [28] at short distances has been applied to ensure the validity of the perturbative matching. However, such a renormalization is still not the perfect choice and there are more systematics to be controlled

*Electronic address: holligan@umd.edu

†Electronic address: xji@umd.edu

‡Electronic address: hueywen@msu.edu

§Electronic address: ysu12345@umd.edu

¶Electronic address: rayzhang@umd.edu

including the power accuracy, the large logarithms in the perturbative matching kernel and the endpoint region where the LaMET expansion breaks down.

The power accuracy is not automatically guaranteed in LaMET calculations, because of the ambiguity in determining the linear divergence, and the factorially divergent coefficients in the perturbative matching. This ambiguity results in an extra $\mathcal{O}(\Lambda_{\text{QCD}}/xP_z)$ leading power correction to the matching procedure. These have previously been handled by absorbing their behavior into a single fit parameter (often denoted m_0) when the lattice matrix elements are renormalized, while still using a fixed-order matching kernel. However, this method was examined in Ref. [29] and found to be flawed. The same paper describes a more robust method, known as leading-renormalon resummation (LRR), defining a renormalization scheme of the linear divergence in the perturbative results by resumming the contribution from fermion loops and tadpole diagrams. Then the non-perturbative parameter m_0 can be extracted reliably to match the renormalized lattice data to $\overline{\text{MS}}$ perturbative calculations to linear z accuracy. A corresponding LRR correction to the matching kernel eliminates the ambiguity from renormalization and thus improves the accuracy to $\mathcal{O}(\Lambda_{\text{QCD}}/xP_z)$. We demonstrate in this work that the renormalization with LRR significantly improves the behavior of the quasi-DA short-distance correlations, making the results more consistent with the theoretical prediction from the operator product expansion (OPE).

The factorization of LaMET observables includes both the nonperturbative lightcone distributions and the perturbative matching. The perturbative matching always involves logarithms of the renormalization scale μ and the physical scale of the system. When the logarithm becomes large, the higher-order effects are no longer negligible, and these higher-order logs need to be rearranged to ensure convergence of the perturbation series. This can usually be done by setting the renormalization scale μ equal to the physical one to eliminate the large logarithms, then solving the renormalization group (RG) equations to recover the μ dependence. This is known as renormalization-group resummation (RGR). When the physical scale becomes too small (around Λ_{QCD}), we reach the Landau pole, which suggests that perturbation theory breaks down or contains very large uncertainties. In the case of the parton distribution function (PDF), the only physical momentum is the parton momentum xP_z , so the logarithms become large at small x . Its effects and importance have been discussed in a recent work [30]. The case of DAs is slightly different, as two different physical scales emerge. One scale is the quark momentum xP_z , and the other is the antiquark momentum $(1-x)P_z$. The existence of two different but correlated scales makes it more complicated to apply RGR because no choice of μ can eliminate the large logarithms simultaneously. In coordinate space, there is only one physical scale, the inverse of the correlation length z^{-1} . Thus, in principle it is easier to implement RGR in coordinate

space for DAs. The coordinate-space matching is based on the short-distance twist expansion, which no longer works after reaching the Landau pole at $z \sim \Lambda_{\text{QCD}}^{-1}$. This prevents us from extracting the x dependence of the DAs with coordinate-space matching. To obtain the lightcone DA with RGR, we propose a phenomenological approach to resum the two logs simultaneously, which is valid in the mid- x region, where LaMET gives accurate predictions.

In principle, the endpoint regions are not calculable from LaMET, because its applicable range is just the mid- x region $x \in [x_{\text{min}}, x_{\text{max}}]$ where $x_{\text{min}} \sim \Lambda_{\text{QCD}}/P_z$ and $x_{\text{max}} = 1 - x_{\text{min}}$. However, the short-distance OPE provides us with global information about the lightcone distribution, allowing us to determine a few lowest moments of the lightcone DA, but not the local x -dependence. The two methods complement each other [31], enabling us to combine the local information from the LaMET calculation and the global information from the short-distance OPE. We model the x -dependence outside the region $x \in [x_{\text{min}}, x_{\text{max}}]$ and fit to the short-distance correlations, obtaining a model-independent mid- x distribution and a model-dependent endpoint distribution. The endpoint distribution is constrained by the physical requirement $\phi(x) \rightarrow 0$ when $x \rightarrow 0$ or 1 as well as the requirement of continuity with the LaMET calculation, which limit the model dependence. This combined approach provides a full x -dependence calculation.

With the above three ideas (elimination of the linear correction, resummation of large logarithms and constraining the endpoint regions), we improve the analysis of the lattice quasi-DA data to extract the full x -dependence of the lightcone DA with high accuracy. The rest of the article is arranged as follows. In Sec. II, we describe the DA calculation using LaMET, discuss the ambiguities in the renormalization and perturbative matching, and present how we achieve power accuracy in the LaMET matching. In Sec. III, we discuss the origin of two different physical scales in the LaMET matching and show how to resum them. In Sec. IV, we discuss how to use the short-distance OPE to constrain the endpoint regions to extend our calculation to the full range of x . In Sec. V, we apply LRR renormalization and LRR matching with RGR to extract the lightcone DA, then use complementarity to obtain the full x dependence. Finally, we conclude in Sec. VI. Due to the abundance of notation in this paper, we tabulate the various symbols in appendix A in addition to defining them as they are introduced in the main sections. In appendix B, we provide a numerical implementation of the RGR method proposed for DA matching. In appendix C, we show more technical details on how to modify the matching kernel with LRR to reach power accuracy.

II. RENORMALIZATION AND POWER ACCURACY

The correlator that defines the pion DA on the lightcone is

$$\phi_\pi(x, \mu) = \int \frac{d\eta^-}{2\pi} e^{ixP^+\eta^-} \langle 0 | \bar{\psi}(0) \gamma_5 \gamma_z W(0, \eta^-) \psi(\eta^-) | \pi(P) \rangle, \quad (1)$$

where $W(0, \eta^-) = \hat{P} \exp \left[-ig \int_0^{\eta^-} ds n_\mu A^\mu(ns) \right]$ is the Wilson line between the two points 0 and η^- , and \hat{P} is the path-ordering operator. Lightcone coordinates are defined for a general Lorentz vector V^μ , as $V^\pm = \frac{1}{\sqrt{2}}(V^0 \pm V^3)$, since we may assume without loss of generality that the meson is traveling in the z ($\equiv \eta^3$) direction. The term g is the coupling, A^μ denotes the gauge field and $|\pi(P)\rangle$ is a pion state with 4-momentum P^+ . The variable x is the fraction of the meson momentum carried by the constituent parton.

The operator in Eq. (1) has dependence on real time and is, thus, inaccessible on the lattice. The method of LaMET begins with the following ‘‘quasi’’ correlation:

$$\begin{aligned} \tilde{\phi}_\pi(x, P_z) &= \int \frac{dz}{2\pi} e^{ixP_z z} \tilde{h}_\pi^R(z, P_z) \\ &= \int \frac{dz}{2\pi} e^{ixP_z z} \langle 0 | \bar{\psi}(0, \vec{0}) \gamma_5 \gamma_z W(0, z) \psi(0, \vec{z}) | \pi(P_z) \rangle_R, \end{aligned} \quad (2)$$

where \tilde{h}_π^R is the renormalized coordinate-space matrix element defined in the second line. The lightcone DA, $\phi_\pi(x, \mu)$, is related to the quasi-DA (qDA) via

$$\begin{aligned} \tilde{\phi}_\pi(x, P_z) &= \int_0^1 dy \phi_\pi(y, \mu) \mathcal{C}(x, y, \mu, P_z) \\ &+ \mathcal{O} \left(\frac{\Lambda_{\text{QCD}}^2}{x^2 P_z^2}, \frac{\Lambda_{\text{QCD}}^2}{(1-x)^2 P_z^2} \right), \end{aligned} \quad (3)$$

where the $\mathcal{C}(x, y, \mu, P_z)$ is the perturbative matching kernel in momentum space, and the residual quadratic in Λ_{QCD}/P_z in the second line comes from higher-twist effects.

The bare matrix elements we compute on the lattice are the $\tilde{h}_\pi^B(z, P_z, a)$ terms corresponding to Eq. (2) before renormalization, so our data are initially in position space and contain UV divergences. The spatial Wilson line $W(0, z)$ has a linearly-divergent self energy of size $\frac{1}{a}$, so it must be removed through a multiplicative renormalization [32] before extrapolating to the continuum.

$$\tilde{h}^R(z, P_z, a) = \tilde{h}^B(z, P_z, a) / Z_R(z, a), \quad (4)$$

where $Z_R(a, z) \sim e^{-\delta m(a)z}$ is the renormalization constant with the linearly divergent mass counterterm $\delta m(a)$.

When expanding $\delta m(a)$ as a perturbation series in the strong coupling, α_s ,

$$\delta m = \frac{1}{a} \sum_n r_n \alpha_s^{n+1} (a^{-1}), \quad (5)$$

the coefficient $r_n \sim n!$ grows factorially at higher orders [33, 34]. Thus, the series is divergent for any α_s , and the sum is ill-defined. We need to introduce an additional renormalization scheme for the linear divergence to define $\delta m(a, \tau)$ unambiguously, with a new τ -dependence. This result varies by $\mathcal{O}(\Lambda_{\text{QCD}})$ in different τ -schemes, so an ambiguity of $\mathcal{O}(z\Lambda_{\text{QCD}})$ arises in the renormalization factor. The same intrinsic ambiguity appears when we try to extract δm from fitting lattice data, where δm is always mixed with another non-perturbative quantity, such that we have a freedom to choose among different fitting results. Similarly, a calculation of the perturbative matching kernel $\mathcal{C}(x, y, \mu, P_z)$ suggests the same factorial growth [35]. The lightcone distribution $\phi(x, \mu)$ is obtained by convolving the inverse matching kernel $\mathcal{C}^{-1}(x, y, \mu, P_z)$ with the renormalized quasi-DA, $\tilde{\phi}_\pi(x, P_z)$, both containing the ambiguities. The combination will in general result in a linear correction $\mathcal{O}\left(\frac{\Lambda_{\text{QCD}}}{xP_z}\right)$ to the matching [27],

$$\begin{aligned} \tilde{\phi}_\pi(x, P_z) &= \int_0^1 dy \phi(y, \mu) \mathcal{C}(x, y, \mu, P_z) \\ &+ \mathcal{O} \left(\frac{\Lambda_{\text{QCD}}}{xP_z} \right) + \mathcal{O} \left(\frac{\Lambda_{\text{QCD}}^2}{x^2 P_z^2} \right), \end{aligned} \quad (6)$$

where we have ignored the $(1-x)P_z$ scale for simplicity, which can be recovered by a substitution $x \leftrightarrow 1-x$, due to the symmetry of the matching. When the hadron momentum is large enough, this correction is not important. But the hadron states in lattice calculations are usually moving with $P_z \sim \text{GeV}$, where the linear correction is not negligible, especially near the endpoints, and more important than the quadratic higher-twist effects.

In principle, these ambiguities from the two pieces can cancel because the twist-2 lightcone DA $\phi(x, \mu)$ is free of linear divergence. Thus, the power accuracy up to $\mathcal{O}\left(\frac{\Lambda_{\text{QCD}}}{xP_z}\right)$ is the best we can achieve without knowing higher-twist information. It has been proven that they indeed cancel only when the linear divergences are renormalized in the same τ -scheme [29]. To achieve this accuracy, we need to carefully define the renormalization scheme for the linear divergence δm and the perturbative matching to eliminate the linear correction.

A recent work [23] uses a fixed-order approach to handle this ambiguity by introducing an additional parameter, denoted by m_0 , in the renormalization process to ensure that the short-distance behavior of the renormalized matrix element is in agreement with perturbation theory. The approach is still not good enough for several reasons: 1) A bridge is missing to connect the lattice calculation and the perturbative calculation, usually known

as the scheme-conversion factor in the renormalization; 2) Resumming the logarithms $\ln(z^2\mu^2)$ at short distances clearly suggests that m_0 is not a constant but has a large dependence on z , mainly due to the fixed-order truncation not being a proper scheme to renormalize the divergent series [29]; 3) A fixed-order matching is used, which cannot eliminate the linear ambiguity.

We propose a new approach, aimed at eliminating such a correction to achieve the power accuracy, as demonstrated in Ref. [29]. It includes three steps:

- Extract the m_0^{eff} parameter by requiring that the lattice data renormalized in τ' -scheme differ from the LRR-improved perturbative calculations in τ -scheme by a factor $\exp(m_0^{\text{eff}}z)$ at short distance;
- Renormalize the $P_z > 0$ lattice data with the renormalization factors extracted from the previous step in τ -scheme;
- Modify the perturbative matching kernel with the same LRR-improvement in τ -scheme.

We choose to extract the m_0^{eff} parameter from $P_z = 0$ pion quasi-PDF data and use it for the renormalization of the quasi-DA at nonzero momentum. The justification for this is that the linear divergence is independent of the external state and the Dirac structure. δm is universal for the Wilson-line self energy, which is exactly the same in these observables ($P_z = 0$ and $P_z \neq 0$) obtained from the same gluon action; the leading β_0 tadpole diagrams that we resum in the $\overline{\text{MS}}$ perturbative calculation are the same for these operators, up to an overall phase factor depending on the external states' momentum. Thus, once the cancellation of the ambiguities is achieved for the one observable, it is also guaranteed for other observables of a similar structure, i.e., with the same Wilson line in the quark bilinear operator but with a different Dirac structure or different external states.

The LRR affects the renormalization in two ways. Firstly, the $e^{m_0^{\text{eff}}z}$ factor is extracted with LRR, so it is different from that extracted in fixed-order perturbation theory, and will have a much smaller uncertainty. Secondly, in the hybrid scheme, we divide the renormalized matrix element by $P_z = 0$ perturbative results (i.e., the Wilson coefficient C_{00}) at short distance, which has a slightly different z dependence after LRR. The renormalized matrix element is expected to be described by the OPE at short distance, with the lowest few moments as inputs. This moment is supposed to be consistent with the one extracted from a renormalization-independent ratio between two different momenta, which will be discussed in more detail in Sec. IV. Thus, a comparison between the moments extracted from the renormalization-dependent matrix element and from the renormalization-independent ratio will test whether the renormalization is properly done.

III. SMALL MOMENTUM LOG RESUMMATION

A. Resummation in coordinate space

To study the resummation of large logarithms, we start from a simpler case, the coordinate-space matching of the quasi-DA. It is more straightforward because only one physical scale, $z = \lambda/P_z$, is involved in the matching. The renormalized quasi-DA matrix element, $\tilde{h}^R(\lambda, P_z)$, can be matched to lightcone DA, $h(\lambda, \mu)$, through

$$\tilde{h}^R(\lambda, P_z) = \int_0^1 d\nu h(\nu\lambda, \mu) \mathcal{Z}(\nu, z^2, \mu^2, \lambda) + \mathcal{O}(z^2 \Lambda_{\text{QCD}}^2), \quad (7)$$

where $\mathcal{Z}(\nu, z^2, \mu^2, \lambda)$ is the perturbative matching kernel in coordinate space. In the ratio scheme [36–38],

$$\begin{aligned} \mathcal{Z}(\nu, z^2, \mu^2, \lambda) = & \delta(1-\nu) \\ & + \frac{\alpha_s C_F}{2\pi} \left\{ \left(\frac{\nu}{1-\nu} \right)_+ \left(-(1+L)(1+e^{-i\lambda(1-\nu)}) \right) \right. \\ & - 2 \left(\frac{\ln(1-\nu)}{1-\nu} \right)_+ (1+e^{-i\lambda(1-\nu)}) \\ & \left. + \left(\frac{1-e^{-i\lambda(1-\nu)}}{i\lambda} - \frac{1}{2}\delta(1-\nu) \right) (3-L) \right\}, \quad (8) \end{aligned}$$

where $L = \ln(z^2\mu^2 e^{2\gamma_E}/4)$ is the only scale-dependent logarithm appearing in the kernel and C_F is the quadratic Casimir for the fundamental representation of $\text{SU}(3)$. At either short distance, $z \rightarrow 0$, or long distance, $z \gg \Lambda_{\text{QCD}}^{-1}$, the logarithm becomes large. We can eliminate the logarithm by setting $\mu_0 = 2e^{-\gamma_E} z^{-1}$ on the right-hand side of the equation. Then an RG evolution to the default scale, e.g. $\mu = 2 \text{ GeV}$, will resum the large logarithms at that scale,

$$\begin{aligned} \tilde{h}^R(\lambda, P_z) = & \int_0^1 d\nu \exp \left[\int_\mu^{\mu_0} \hat{\mathcal{V}}(\rho/\nu, \lambda, \mu') d \ln \mu'^2 \right] \\ & \times h(\rho\lambda, \mu) \mathcal{Z}(\nu, z^2, \mu_0^2, \lambda) + \mathcal{O}(z^2 \Lambda_{\text{QCD}}^2), \quad (9) \end{aligned}$$

where $\hat{\mathcal{V}}$ is the coordinate space representation of the Efremov-Radyushkin-Brodsky-Lepage (ERBL) evolution kernel [39–42],

$$\begin{aligned} \hat{\mathcal{V}}(\nu, \lambda, \mu) = & \frac{\alpha_s(\mu) C_F}{2\pi} \left((1+e^{-i\lambda(1-\nu)}) \left(\frac{\nu}{1-\nu} \right)_+ \right. \\ & \left. + \left(\frac{1-e^{-i\lambda(1-\nu)}}{i\lambda} - \frac{1}{2}\delta(1-\nu) \right) \right) \theta(1-\nu). \quad (10) \end{aligned}$$

Both the evolution and matching kernels can be made purely real by multiplying by a phase factor $e^{i\lambda(1-\nu)/2}$, and apply to the phase-rotated matrix elements

$$\tilde{H}^R(\lambda, P_z) = e^{i\lambda/2} \tilde{h}^R(\lambda, P_z), \quad (11)$$

which is purely real for symmetric DAs that satisfy $\phi(x) = \phi(1-x)$. So the matching and the evolution preserve the symmetry of the DAs.

Such a resummation works fine at short distances, but at long distances the scale μ_0 hits the Landau pole, indicating that the perturbation theory as well as the entire short-distance operator expansion break down. Without knowing the correct information at large z , we are unable to extract the x dependence of the DA.

B. Origin of two different scales

To avoid the nonperturbative long-tail issue in coordinate space, we can choose to perform the resummation and matching in momentum space, leaving the problem to the endpoint region $x \rightarrow 0$ and $x \rightarrow 1$. In momentum space, the quasi-DA is matched to the lightcone DA through

$$\tilde{\phi}(x, P_z) = \int_0^1 dy \mathcal{C}(x, y, \mu, P_z) \phi(y, \mu) + \mathcal{O}\left(\frac{\Lambda_{\text{QCD}}^2}{y(1-y)P_z^2}\right). \quad (12)$$

The momentum-space matching kernel $\mathcal{C}(x, y, \mu, P_z)$ can be obtained from a double Fourier transformation of the coordinate-space matching in Eq. (8),

$$\mathcal{C}(x, y, \mu, P_z) = \int_{-\infty}^{\infty} \frac{d\lambda}{2\pi} e^{ix\lambda} \int_0^1 d\nu e^{-i\nu y\lambda} \mathcal{Z}\left(\nu, \frac{\lambda^2}{y^2 P_z^2}, \mu^2\right). \quad (13)$$

To trace how the physical scale and the logarithm transform, we can check the double Fourier transform of the logs, L , in $\mathcal{Z}(\nu, \frac{\lambda^2}{y^2 P_z^2}, \mu^2)$ of Eq. (8). The terms involved include $f(\nu)L$ and $f(\nu)L e^{-i\lambda(1-\nu)}$. In dimensional regularization $d = 4 - 2\epsilon$, higher-order logs L^n can be expressed as the $\mathcal{O}(1)$ term of $\frac{n!}{\epsilon^n} (\mu^2 z^2 e^{2\gamma_E}/4)^\epsilon$ in the ϵ expansion. Integrating λ first, we obtain

$$\begin{aligned} & \int_{-\infty}^{\infty} \frac{d\lambda}{2\pi} e^{ix\lambda} \int_0^1 d\nu e^{-i\nu y\lambda} \frac{n! f(\nu)}{\epsilon^n} \left(\frac{\lambda^2 \mu^2 e^{2\gamma_E}}{4P_z^2}\right)^\epsilon \\ &= \int_0^1 \frac{d\nu f(\nu) n!}{|x-y\nu|^{1+2\epsilon}} \frac{\Gamma(1/2+\epsilon)}{\sqrt{\pi}\epsilon^n \Gamma(-\epsilon)} \left(\frac{\mu^2 e^{2\gamma_E}}{P_z^2}\right)^\epsilon \\ &= \int_0^1 \frac{d\nu f(\nu) n!}{y|x/y-\nu|^{1+2\epsilon}} \frac{\Gamma(1/2+\epsilon)}{\sqrt{\pi}\epsilon^n \Gamma(-\epsilon)} \left(\frac{\mu^2 e^{2\gamma_E}}{y^2 P_z^2}\right)^\epsilon, \end{aligned} \quad (14)$$

which can be expanded in $\epsilon \rightarrow 0$ [43]. Note that only when $0 < x/y < 1$ is it possible for $|x/y-\nu|$ to be zero in the integration region $\nu \in [0, 1]$, and then the expansion of $|x/y-\nu|^{-1-2\epsilon}$ generates the leading divergent term $\frac{-1}{2\epsilon} \delta(x/y-\nu)$. So when x is in the nonphysical region, or when $1 > x > y > 0$, the expansion does not contain any leading logarithms of $(\ln \mu)^n$. When $0 < x < y < 1$, the

expansion yields additional log terms

$$\begin{aligned} & \int_0^1 d\nu f(\nu) (\ln^n(\mu^2) - n \ln^{n-1}(\mu^2) \ln(4y^2 P_z^2)) \\ & \quad \times \delta(x-y\nu) + \mathcal{O}(\ln^{n-2} \mu) \\ &= \int_0^1 d\nu f(\nu) \delta(x-y\nu) \ln^n\left(\frac{\mu^2}{4y^2 P_z^2}\right) + \mathcal{O}(\ln^{n-2} \mu). \end{aligned} \quad (15)$$

The remaining integral preserves the structure of the log but only changes its coefficients. Thus, we get the physical scale $2yP_z$ for this term. On the other hand, the other term $f(\nu)L e^{-i\lambda(1-\nu)}$ after a double Fourier transformation becomes

$$\begin{aligned} & \int \frac{d\lambda}{2\pi} e^{ix\lambda} \int_0^1 d\nu e^{-i\nu y\lambda} e^{-i\lambda(1-\nu)} \frac{n! f(\nu)}{\epsilon^n} \left(\frac{\lambda^2 \mu^2 e^{2\gamma_E}}{4P_z^2}\right)^\epsilon \\ &= \int_0^1 \frac{d\nu f(\nu) n!}{|\bar{x}-\bar{y}\nu|^{1+2\epsilon}} \frac{\Gamma(1/2+\epsilon)}{\sqrt{\pi}\epsilon^n \Gamma(-\epsilon)} \left(\frac{\mu^2 e^{2\gamma_E}}{P_z^2}\right)^\epsilon \\ &= \int_0^1 \frac{d\nu f(\nu) n!}{\bar{y}|\bar{x}/\bar{y}-\nu|^{1+2\epsilon}} \frac{\Gamma(1/2+\epsilon)}{\sqrt{\pi}\epsilon^n \Gamma(-\epsilon)} \left(\frac{\mu^2 e^{2\gamma_E}}{\bar{y}^2 P_z^2}\right)^\epsilon, \end{aligned} \quad (16)$$

with $\bar{x} \equiv 1-x$ and $\bar{y} \equiv 1-y$, which does not contain any leading logarithm when $1-x$ is nonphysical, or when $0 < x < y < 1$. When $1 > x > y > 0$, the ϵ expansion yields

$$\int_0^1 d\nu f(\nu) \delta(\bar{x}-\bar{y}\nu) \ln^n\left(\frac{\mu^2}{4\bar{y}^2 P_z^2}\right) + \mathcal{O}(\ln^{n-2} \mu). \quad (17)$$

So the two different physical scales correspond to different regions of x and y . The scale $2yP_z$ for $x < y$ corresponds to the quark-splitting process; the scale $2(1-y)P_z$ for $x > y$ corresponds to the antiquark-splitting process.

Note that the two scales $2yP_z$ and $2(1-y)P_z$ we obtained at the current stage both depend on the convolution variable y , which is, in principle, not implementable because we cannot have different scales μ for different y in $\phi(\mu, y)$. However, note that the matching kernel $\mathcal{C}(x, y, \mu, P_z)$ is almost localized, i.e., the region of $x \sim y$ is greatly enhanced compared to any other regions. As a result, the proper scale choice to resum the RG logarithm would be $2xP_z$ and $2(1-x)P_z$ instead, corresponding to the quark and antiquark momentum fractions in the quasi-DA. Moreover, a comparison between the quasi-PDF and DIS shown in Ref. [30] suggests that $2xP_z$ is the proper scale in the quasi-PDF case, also supports the scales to be $2xP_z$ and $2(1-x)P_z$ in our quasi-DA.

C. Resummation of two different logarithms

The perturbative matching kernel in Eq. (12) $\mathcal{C}(x, y, \mu, P_z) = \delta(x-y) + \mathcal{C}^{(1)}(x, y, \mu, P_z) + \mathcal{O}(\alpha_s^2)$ has been calculated to 1-loop order [44], where $\mathcal{C}^{(1)}$ is the $\mathcal{O}(\alpha_s)$ term of the matching, and satisfies the quark-antiquark symmetry

$$\mathcal{C}(x, y, \mu, P_z) = \mathcal{C}(1-x, 1-y, \mu, P_z). \quad (18)$$

In the two regions $x < y$ and $y < x$, the matching kernel has different μ dependencies, corresponding to the piecewise function of the ERBL evolution kernel:

$$\frac{d\phi(x)}{d\ln\mu^2} = \int_0^1 dy \frac{\alpha_s C_F}{2\pi} V^{(0)}(x, y) \phi(y) + \mathcal{O}(\alpha_s^2), \quad (19)$$

where

$$V^{(0)}(x, y) = \left(\frac{x}{y} \frac{1-x+y}{y-x} \theta(y-x) + \left[\frac{x \leftrightarrow \bar{x}}{y \leftrightarrow \bar{y}} \right]_+ \right), \quad (20)$$

and the plus function is

$$f(x, y)_+ = f(x, y) + \delta(x-y) \int_0^1 dz f(z, y). \quad (21)$$

The logarithms become large in the matching kernel $\mathcal{C}(x, y, \mu, P_z)$ for x close to both endpoints $x \rightarrow 0$ or 1 , so a resummation of large logs is necessary. The traditional method of resummation is to choose a scale μ_0 in the scale-independent factorization such that the large logs in $\mathcal{C}(x, y, \mu_0, P_z)$ are eliminated, and apply the RG evolution of $\phi(y, \mu)$:

$$\begin{aligned} \tilde{\phi}(x, P_z) &= \int_0^1 dy \mathcal{C}(x, y, \mu_0, P_z) \\ &\quad \times \mathcal{P} \exp \left[\int_{\mu}^{\mu_0} \hat{V} d\ln\mu'^2 \right] \phi(y, \mu), \end{aligned} \quad (22)$$

where \mathcal{P} is the path ordering of the evolution path, and \hat{V} is the operator corresponding to the ERBL kernel acting on ϕ . However, such an approach does not work in the quasi-DA's case, because there are two different scales in the piecewise matching kernel. The logarithm in $x < y$ is $\ln[4x^2 P_z^2 / \mu^2]$, corresponding to the quark-splitting; the logarithm in $x > y$ is $\ln[4(1-x)^2 P_z^2 / \mu^2]$, corresponding to the antiquark-splitting. No one choice of μ_0 is able to eliminate the two logs at the same time. We have to develop a different strategy to resum the log in the DA.

We start from separating the matching formula in two different regions

$$\begin{aligned} \tilde{\phi}(x) &= \phi(x, \mu) + \int_{x < y} dy \mathcal{C}^{(1)}(x, y, \mu) \phi(y, \mu) \\ &\quad + \int_{x > y} dy \mathcal{C}^{(1)}(x, y, \mu) \phi(y, \mu) + \mathcal{O}(\alpha_s^2) \\ &= \phi(x, \mu) + \mathcal{C}_L^{(1)}(\mu) \otimes \phi(\mu) + \mathcal{C}_R^{(1)}(\mu) \otimes \phi(\mu), \end{aligned} \quad (23)$$

where we label the integral in two regions as $\mathcal{C}_L^{(1)}$ and $\mathcal{C}_R^{(1)}$ convoluted with ϕ . One idea is to set the two terms to different scales, $\mathcal{C}_L^{(1)}(2xP_z) \otimes \phi(2xP_z)$ and $\mathcal{C}_R^{(1)}(2(1-x)P_z) \otimes \phi(2(1-x)P_z)$. To make this possible, we need to split the first term into two parts and combine with them separately. After the split, the two parts need to be scale-invariant individually up to order α_s . So we need

to find the weights, $w_L(x)$ and $w_R(x) = 1 - w_L(x)$, for the following split

$$\begin{aligned} \tilde{\phi}(x) &= w_L(x) \phi(x, \mu) + \mathcal{C}_L^{(1)}(\mu) \otimes \phi(\mu) \\ &\quad + w_R(x) \phi(x, \mu) + \mathcal{C}_R^{(1)}(\mu) \otimes \phi(\mu), \end{aligned} \quad (24)$$

such that the two lines are individually scale-independent. If we force $w_L(x)$ to be scale independent, then simple algebra gives

$$w_L(x) = \frac{V_L^{(0)} \otimes \phi(\mu)}{V^{(0)} \otimes \phi(\mu)}, \quad (25)$$

where we define $V_L^{(0)} \equiv V^{(0)}|_{x < y}$ and $V_R^{(0)} \equiv V^{(0)}|_{x > y}$ in a similar way. The solution $w_L(x)$ is scale-dependent at order α_s , contradicting our requirement. However, noticing that $\phi(\mu)$ and $\tilde{\phi}$ differ by $\mathcal{O}(\alpha_s)$ corrections, and the quasi-DA $\tilde{\phi}$ is scale independent, we may substitute the $\phi(\mu)$ in Eq. (25) with $\tilde{\phi}$, making $w_L(x)$ scale independent. The new solution

$$w_L(x) = \frac{V_L^{(0)} \otimes \tilde{\phi}}{V^{(0)} \otimes \tilde{\phi}}, \quad (26)$$

satisfies the scale dependence of the original equation at order $\mathcal{O}(\alpha_s)$,

$$\begin{aligned} \frac{dw_L(x)\phi(x)}{d\ln\mu^2} &= \frac{\alpha_s C_F}{2\pi} \frac{V^{(0)} \otimes \phi(\mu) (V_L^{(0)} \otimes \tilde{\phi}(\mu))}{V^{(0)} \otimes \tilde{\phi}(\mu)} \\ &= \frac{\alpha_s C_F}{2\pi} \frac{V^{(0)} \otimes \phi(\mu) (V_L^{(0)} \otimes \phi(\mu)) (1 + \mathcal{O}(\alpha_s))}{V^{(0)} \otimes \phi(\mu) (1 + \mathcal{O}(\alpha_s))} \\ &= \frac{\alpha_s C_F}{2\pi} V_L^{(0)} \otimes \phi(\mu) + \mathcal{O}(\alpha_s^2), \end{aligned} \quad (27)$$

which cancels the μ dependence in $\mathcal{C}_L^{(1)}(\mu) \otimes \phi(\mu)$. So we write the matching formula as

$$\begin{aligned} \tilde{\phi}(x) &= \frac{V_L^{(0)} \otimes \tilde{\phi}}{V^{(0)} \otimes \tilde{\phi}} \phi(x, \mu_1) + \mathcal{C}_L^{(1)}(\mu_1) \otimes \phi(\mu_1) \\ &\quad + \frac{V_R^{(0)} \otimes \tilde{\phi}}{V^{(0)} \otimes \tilde{\phi}} \phi(x, \mu_2) + \mathcal{C}_R^{(1)}(\mu_2) \otimes \phi(\mu_2), \end{aligned} \quad (28)$$

where the two scales are chosen to be $\mu_1 = 2xP_z$ and $\mu_2 = 2(1-x)P_z$ so that the small-momentum logarithms in both $\mathcal{C}_L^{(1)}(\mu_1)$ and $\mathcal{C}_R^{(1)}(\mu_2)$ vanish.

To extract the lightcone-DA at a specific factorization scale μ , we can relate the quasi-DA, $\tilde{\phi}(x)$, to the lightcone DA, $\phi(\mu, x)$, through

$$\begin{aligned} \tilde{\phi} &= \left(\left(\frac{V_L^{(0)} \otimes \tilde{\phi}}{V^{(0)} \otimes \tilde{\phi}} + \hat{\mathcal{C}}_L^{(1)}(\mu_1) \right) \mathcal{P} \exp \left[\int_{\mu}^{\mu_1} \hat{V} d\ln\mu'^2 \right] \right. \\ &\quad \left. + \left(\frac{V_R^{(0)} \otimes \tilde{\phi}}{V^{(0)} \otimes \tilde{\phi}} + \hat{\mathcal{C}}_R^{(1)}(\mu_2) \right) \mathcal{P} \exp \left[\int_{\mu}^{\mu_2} \hat{V} d\ln\mu'^2 \right] \right) \phi(\mu) \\ &= \hat{\mathcal{C}}_{\text{RGR}}(\mu) \phi(\mu), \end{aligned} \quad (29)$$

where \hat{C} and \hat{V} are both operators acting on the function ϕ through a convolution. Once we solve the resummed matching kernel, $\hat{C}_{\text{RGR}}(\mu)$, the lightcone DA can be extracted from the inverse matching,

$$\phi(\mu, x) = \int dy \hat{C}_{\text{RGR}}^{-1}(x, y, \mu, P_z) \tilde{\phi}(y, P_z). \quad (30)$$

IV. CONSTRAINTS FROM SHORT-DISTANCE OPE

LaMET allows us to determine the pion DA in the moderate x -region. The calculation begins to break down when $x \rightarrow 0$ or $x \rightarrow 1$ as shown in Eq. (3). We can, however, determine the global behavior of the pion DA from the short-distance OPE and use this information to constrain the endpoints.

At short distances, the renormalized coordinate space matrix elements can be expanded in terms of the Mellin moments of the DA

$$\langle \xi^n \rangle = \int_0^1 dx \phi_\pi(x, \mu) (2x - 1)^n \quad (31)$$

where $\xi = x - (1 - x) = 2x - 1$, via the OPE,

$$\begin{aligned} \tilde{H}^R(z, P_z) = & \quad (32) \\ & \sum_{n=0}^{\infty} \frac{(-izP_z/2)^n}{n!} \sum_{m=0}^n C_{nm}(z, \mu) \langle \xi^m \rangle + \mathcal{O}(z^2 \Lambda_{\text{QCD}}^2) \end{aligned}$$

where $C_{nm}(z, \mu)$ are the Wilson coefficients, and $\mathcal{O}(z^2 \Lambda_{\text{QCD}}^2)$ are higher twist effects which become relevant at distances $z \gtrsim 0.2$ fm. Fitting the matrix elements at short distances to the relevant Wilson coefficients allows us to determine the Mellin moments, $\langle \xi^n \rangle$. The Mellin moments describe the global information of the DA and, thus, set constraints on the endpoint region once the mid- x distribution is determined. Combined with the physical requirement that $\phi(0) = \phi(1) = 0$, it allows us to obtain the shape of the DA near the endpoints with small model dependence. This is called the ‘‘complementarity’’ between the large momentum expansion and the short distance factorization.

In our DA analysis, we can fit the moments from the following RG invariant and renormalization independent ratio [45]:

$$\begin{aligned} \mathcal{M}(z, P_1, P_2) &= \tilde{H}^B(z, P_1^z) / \tilde{H}^B(z, P_2^z) \\ &= \frac{\sum_{n=0}^{\infty} \frac{(-izP_1^z/2)^n}{n!} \sum_{m=0}^n C_{nm}(z, \mu) \langle \xi^m \rangle}{\sum_{n=0}^{\infty} \frac{(-izP_2^z/2)^n}{n!} \sum_{m=0}^n C_{nm}(z, \mu) \langle \xi^m \rangle}, \quad (33) \end{aligned}$$

which can be truncated at some order because higher moment contributions are negligible. Then with the Wilson coefficients known from the perturbative calculation, a fit to the short-distance ratio $\mathcal{M}(z, P_1, P_2)$ determines the second Mellin moments $\langle \xi^2 \rangle$ independent of the renormalization method. Given the $\phi^L(x, \mu)$ calculated from

LaMET in the mid- x region, we can model the full x -dependence, $\phi^f(x, \mu)$, as

$$\phi^f(x, \mu) = \begin{cases} \phi^L(x_0, \mu) x^m / x_0^m & 0 \leq x \leq x_0 \\ \phi^L(x, \mu) & x_0 \leq x \leq 1 - x_0 \\ \phi^L(x_0, \mu) \bar{x}^m / \bar{x}_0^m & 1 - x_0 \leq x \leq 1 \end{cases} \quad (34)$$

where x_0 is the minimal x we can calculate with LaMET. Then we can determine the parameter m by requiring

$$\int_0^1 dx \phi^f(x, \mu) (2x - 1)^2 = \langle \xi^2 \rangle_{\text{OPE}}(\mu) \quad (35)$$

to obtain the full distribution.

An alternative approach is not to constrain the endpoint region with moments, but with short distance correlations. Constructing the same full x -range distribution $\phi^f(x, \mu)$, we can first Fourier transform it to coordinate space

$$h^f(z, P_z, \mu) = \int_0^1 dx e^{ixzP_z} \phi^f(x, \mu), \quad (36)$$

then use the short-distance factorization in Eq. (7) to convert it to the quasi-DA correlations $\tilde{h}^f(z, P_z, \mu)$, and fit to our renormalized matrix elements $\tilde{h}(z, P_z, \mu)$. This approach depends on the renormalization of our matrix elements in coordinate space, but not on the data at other momenta.

We expect the second approach to give the same result as the first one. The two approaches provide a consistency check for our renormalization method with the short-distance OPE.

V. NUMERICAL RESULTS

In this work, we re-analyze the data presented in Ref. [21], measured on three lattice ensembles of lattice spacings $a = \{0.0582(4), 0.0888(8), 0.1207(11)\}$ fm and pion mass $m_\pi \approx 310$ MeV generated by the MILC collaboration [46]. The analysis starts with the same bare matrix elements extracted from a two-state fit to the lattice correlators.

A. Renormalization

The method used in Ref. [21] for renormalization was the regularization-independent momentum subtraction scheme (RI/MOM). However, this method has some problems when dealing with the linear divergence in the nonlocal operator with a spatial Wilson line, as well as generating unknown nonperturbative effects at large distances [47]. We deal with these issues by working in the hybrid scheme [27] with the LRR-improved ratio scheme at short distances from the self-renormalization [28], as discussed in the previous section. The renormalization

factors $Z_R(z, a)$ at short distances are obtained from $P_z = 0$ matrix elements of the pion PDF to remove the linear divergence,

$$Z_R(z, a) \equiv \exp \left\{ \Delta\mathcal{I} + \frac{k}{a \ln(a\Lambda_{\text{QCD}})} - m_0^{\text{eff}} z + f(z)a + \frac{3C_F}{4\pi\beta_0} \ln [\ln(1/a\Lambda_{\text{QCD}})] + \ln \left[1 + \frac{d}{\ln(a\Lambda_{\text{QCD}})} \right] \right\} \quad (37)$$

where $\Delta\mathcal{I}$ is a conversion constant in different schemes, adjusted through fitting to make sure the small z -correlations are matched to $\overline{\text{MS}}$ results. The fitting parameter $d = -0.53$ represents the NLO RG evolutions on lattice. The term $\frac{k}{a \ln(a\Lambda_{\text{QCD}})}$ is the linear divergence with fitting parameters k and Λ_{QCD} which are not uniquely determined due to the intrinsic ambiguity. By choosing an arbitrary set of fitting parameters $k = 3.3 \text{ fm}^{-1} \text{ GeV}^{-1}$ and $\Lambda_{\text{QCD}} = 0.1 \text{ GeV}$ [28] as scheme τ' , we can determine a corresponding $m_0^{\text{eff}} = 0.189$ [29] to relate the $P_z = 0$ lattice matrix elements to the perturbative calculation of $C_{00}^{\text{LRR}}(z, \mu, \tau)$, as defined in Appendix C which eliminates such an ambiguity, $f(z)a$ as a fit parameter incorporates the discretization effects and the remaining terms come from the resummed logarithmically divergent dependence on a .

After removing the linear UV divergences through Eq. (4), we are able to extrapolate to the continuum limit to take out additional discretization effects at finite P_z , which is a simple process of fitting the renormalized matrix elements at different lattice spacings but at a fixed z value to a linear function:

$$\tilde{H}^R(z_0, a, P_z) = c(z) \times a + \tilde{H}^R(z_0, a = 0, P_z). \quad (38)$$

for some function $c(z)$ where \tilde{H}^R is defined in Eq. (11). We carry out this extrapolation for a continuous curve after interpolating our data on three lattice spacings. The matrix element after renormalization and continuum

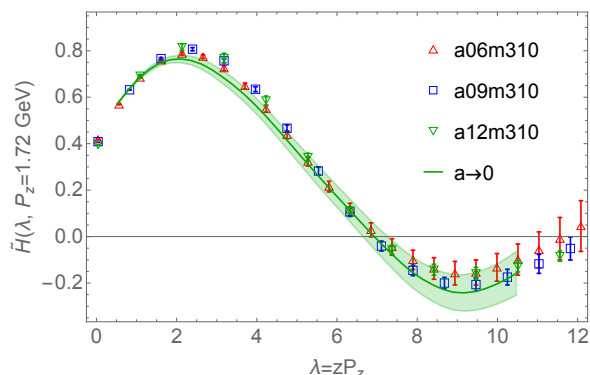


FIG. 1: The continuum extrapolation for renormalized phase rotated matrix elements at $P_z = 1.72 \text{ GeV}$. For the pion, the phase rotated matrix elements are purely real. There is a good consistency among different ensembles, so the continuum extrapolation works fine.

extrapolation is shown in Fig. 1, which shows a good consistency among different lattice spacings. A comparison of renormalized matrix elements \tilde{H}^R at different momenta with the LRR perturbative result at $P_z = 0$ is shown in Fig. 2. We can clearly see that the distribution approaches the $P_z = 0$ perturbative calculations $C_{00}^{\text{LRR}}(z, z^{-1})$ when the momentum decreases.

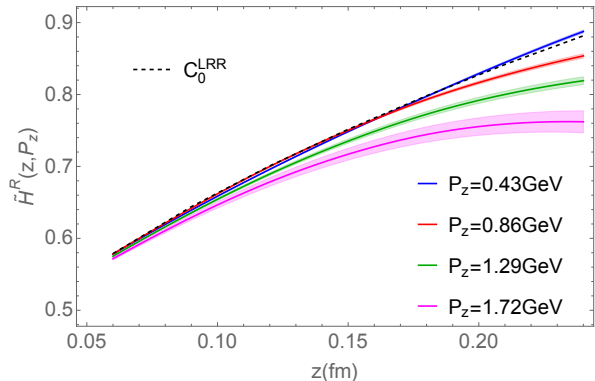


FIG. 2: The renormalized matrix elements for different momenta. As the momentum decreases, the distribution approaches the $P_z = 0$ perturbative calculations $C_{00}^{\text{LRR}}(z, z^{-1})$.

Then a ratio to the $P_z = 0$ perturbative results for DA is taken at short distance $|z| < z_s$ to convert to the hybrid scheme,

$$\mathcal{M}^{\text{hybrid}}(z, P_z, 0) = \frac{\tilde{H}^R(z, P_z)}{\tilde{H}^R(z, P_z = 0)} \theta(z_s - |z|) + \frac{\tilde{H}^R(z, P_z)}{\tilde{H}^R(z_s, P_z = 0)} \theta(|z| - z_s). \quad (39)$$

where \tilde{H}^R is defined in Eq. (11). The parameter z_s that separates the nonperturbative and perturbative regions must be much larger than the lattice spacing to avoid discretization effects but not so large as to necessitate higher-twist terms in the OPE. In our calculations, we choose $z_s = 0.18 \text{ fm}$.

Figure 3 shows a comparison between the ratio $\mathcal{M}^{\text{hybrid}}(z, P_z, 0)$ obtained from fixed-order self-renormalization and the LRR-improved self-renormalization. An obvious problem in the fixed-order renormalization is the hump near $z = 0.1 \text{ fm}$, which suggests a negative second moment $\langle \xi^2 \rangle < 0$, irreconcilable with the OPE predictions at short distance. The LRR-improved renormalized matrix elements, on the other hand, show good consistency with OPE predictions at short distances. This comparison demonstrates that the modification from LRR is necessary for a correct renormalization. Both the continuum extrapolation and the conversion to the hybrid scheme are linear, thus the two steps commute with each other.

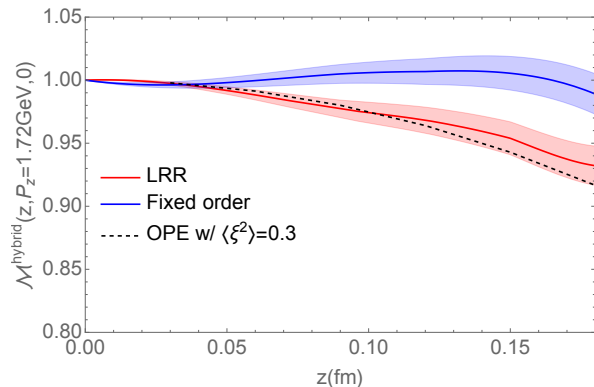


FIG. 3: A comparison between the fixed-order self-renormalization and the LRR-improved self-renormalization. The LRR improves the short distance behavior to be more consistent with the OPE predictions.

B. Extracting x -dependence of quasi-DA

In order to Fourier transform our coordinate space correlations to momentum space to extract the x -dependence, we need to extrapolate our matrix elements to infinite distance. We first convert our position-space variable to Ioffe time $\lambda \equiv zP_z$ as introduced in Sec. III A. Since P_z is fixed for a single calculation, large distance corresponds to large λ . Although the large- λ correlation becomes extremely noisy at a finite momentum from the lattice, which in principle makes it impossible for us to know the longtail information, the distribution is not arbitrary. The quantity we are calculating has its own physical meaning as a momentum distribution and, thus, must follow constraints in momentum space. Such a constraint suggests an algebraic decay along with an exponential decay when converted to coordinate space, and constrains the long-range correlations of the lattice data [23, 27]. The constraints allow us to reduce the error in the large- λ region and extract the x -dependence of the quasi-DA.

Based on these constraints, we can extrapolate our matrix elements in position space to the corresponding inverse Fourier transform [23, 27]:

$$\tilde{H}^R(\lambda \rightarrow \infty, P_z) = \left(e^{i\lambda/2} \frac{c_1}{(i\lambda)^n} + e^{-i\lambda/2} \frac{c_1}{(-i\lambda)^n} \right) e^{-|\lambda|/\lambda_0} \quad (40)$$

where λ_0 is a large constant describing the correlation length and depends on the hadron momentum, and the terms (c_1, n) are fitting parameters. Note that at long distances in our hybrid scheme, the ratio $\mathcal{M}^{\text{hybrid}}(\lambda, P_z)$ only differs from $\tilde{H}^R(\lambda, P_z)$ by a constant factor $\tilde{H}^R(z_s, 0)$, so they have the same functional form. We then fit the longtail of $\mathcal{M}^{\text{hybrid}}(\lambda, P_z)$ to Eq. (40). An example of the large- λ extrapolation is shown in Fig. 4.

With a full-range coordinate space correlation, we are able to extract $\tilde{\phi}(x, P_z)$ through a Fourier transformation

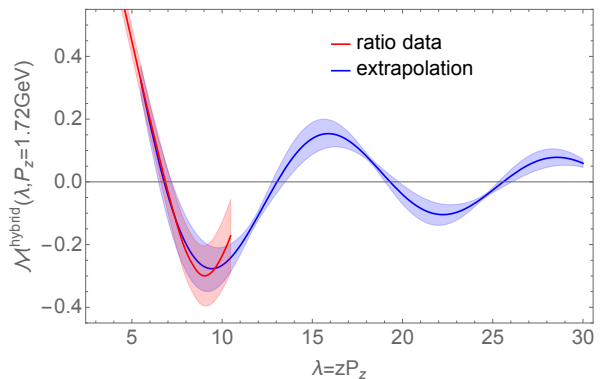


FIG. 4: Continuum position space ratio in the hybrid scheme, $\mathcal{M}(\lambda)$, with extrapolations to large- $|\lambda|$. The consistency between the data (red) and the extrapolation (blue) in the overlapping region suggests the good quality of the extrapolation.

in our chosen renormalization scheme,

$$\tilde{\phi}_\pi(x, P_z) = \int_{-\infty}^{\infty} \frac{d\lambda}{2\pi} e^{ix\lambda} \mathcal{M}^{\text{hybrid}}(\lambda, P_z) \quad (41)$$

as shown in Fig. 5.

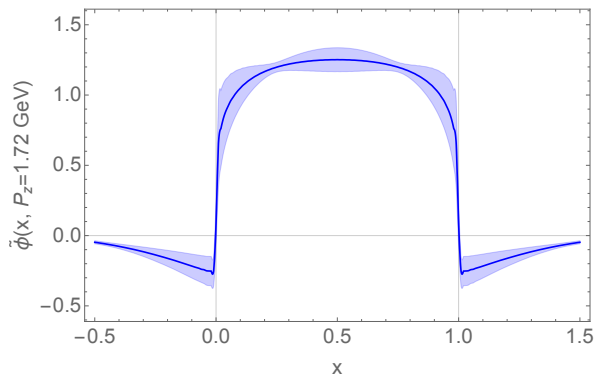


FIG. 5: The x -dependence of the quasi-DA. There is a non-vanishing distribution outside the physical region $x \in [0, 1]$ for the quasi-DA. This nonphysical distribution will be suppressed when matched to the lightcone.

C. Full x -dependence for lightcone DA

After obtaining the quasi-DA in momentum space, we can then apply the inverse matching to obtain the lightcone DA. Firstly, we apply the fixed-order matching kernel, modified with LRR, at scale $\mu = 2$ GeV without the large log resummation. The fixed order matching appears to be valid for the full x region. However, as we discussed, it is just an artificial effect. As we approach the endpoints, the higher-order large logs can no longer be neglected and have to be resummed. We thus apply the matching with RGR, and show the comparison in Fig. 6. The resummed matching causes a divergence at

small physical scales, suggesting that the endpoint region is not accessible in perturbation theory. So we only show a segment of $x \in [0.23, 0.77]$ for the RGR matched result, and use a gray band to shade the outside regions. The RGR effect is almost zero near $x = 0.5$, and starts to suppress the distribution when approaching the endpoints.

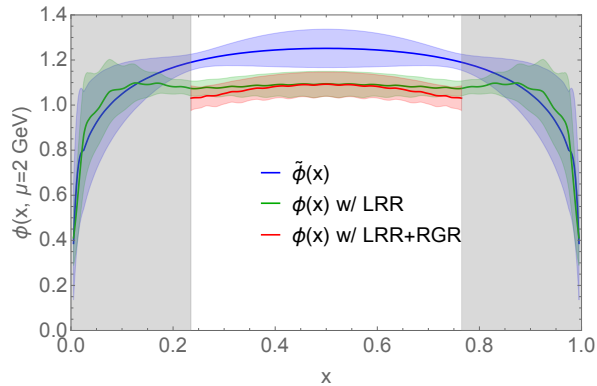


FIG. 6: The mid- x dependence of the lightcone DA after we perform the inverse matching on the quasi-DA $\phi(x)$. The blue band is the quasi-DA $\tilde{\phi}(x)$ before matching as a reference. We show only $x \in [0.23, 0.77]$ for the result with RGR because the strategy does not work outside the range.

Now we have the distribution determined for the mid- x region, while the endpoint regions are still unknown from the LaMET approach. Fortunately, in coordinate space, the small- z region is perturbative, thus, can be resummed safely, and contains the global information of the x -dependent DA, such as its moments. With the information from the mid- x region, we can complete our picture of the extracted DA by utilizing the small- z information to constrain the endpoint behavior, as suggested in Ref. [31].

Near the endpoints, we can parametrize the DA as a power of x or $1-x$ as in Eq. (34). To ensure continuity, we require that the parametrized form coincide with our mid- x results at $x = x_0$. We convert this parametrized DA into coordinate space, apply the short-distance matching, and fit the result to our renormalized matrix elements. Figure 7 shows the comparison from the parametrized DA and our lattice data at short distances, which suggests good consistency. Besides that, we allow some model-dependence by adding a small correction,

$$\phi(x < x_0) = Ax^m(1 + \sin(b)x), \quad (42)$$

where $\sin(b)$ is to guarantee that the size of this correction term is not so large as to cause a sharp turn at the junction point, i.e., the different regions are smoothly connected. The same modification is symmetrically applied to $x \rightarrow 1-x$, and a model-dependence is included as the systematic error by calculating the difference between the modified model and the original one in Eq. (34). The final estimation taking into account such a systematic error is shown in Fig. 8.

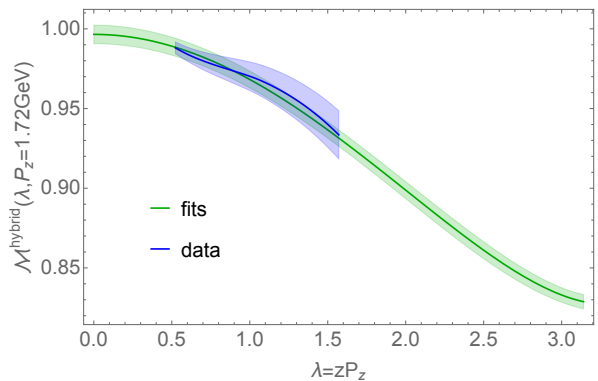


FIG. 7: The fitting of parametrized DA to lattice data at short distance. The fitted short-distance correlations agree well with the data.

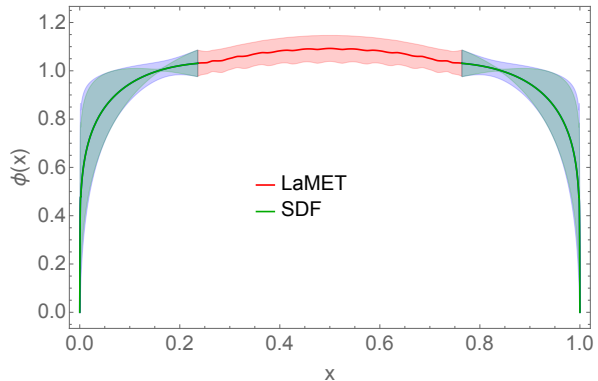


FIG. 8: Full x dependence of the DA. The red band in $x \in [0.23, 0.77]$ is obtained from LaMET, and the green (blue) band is obtained from the short-distance correlations by modeling of the endpoints with statistical (statistical and systematic) errors.

We can estimate the moment from the full x -dependence from Eq. (31) with Eq. (34). We get

$$\langle 1 \rangle = 0.996(6), \quad \langle \xi^2 \rangle = 0.302(23), \quad (43)$$

which are in good agreement with the theoretical normalization $\langle 1 \rangle = 1$, and the second moment $\langle \xi^2 \rangle = 0.298(39)$ obtained from the renormalization-independent OPE fit to Eq. (33). This is strong support for our renormalization method.

The second Mellin moment we obtained from the renormalization independent ratio and from the final full x -dependence, although self-consistent, are significantly greater than the latest calculation of local twist-2 operators $\langle \xi^2 \rangle = 0.234(8)$ [11]. Can we reconstruct the short distance correlations based on the moment $\langle \xi^2 \rangle = 0.234(8)$ calculated from local twist-2 operators, while keeping the long distance correlations from our lattice calculation, and apply the same procedure of analysis to get a full x -dependent distribution? Our analysis on the original data suggests a good self-consistency. Will we also see the similar consistency of $\langle \xi^2 \rangle \sim 0.234(8)$ by

reconstructing the short-distance correlation from OPE? The answer is no. Only modifying the small- λ region seems to change the moments in the lightcone DA, but this kind of modification spreads over the entire momentum space of $x \in [-\infty, \infty]$, not limited in the physical region. The non-vanishing modification to the non-physical region contributes to most of the moment difference, indicating that it is not consistent by just correcting the small- λ correlation with OPE. The inconsistency appears as a bad fit to the small- λ correlation when we use the complementarity to complete the endpoint regions.

In Fig. 9 we compare with previous model-dependent calculations and lattice results, including the Dyson-Schwinger Equation (DSE'13) [48], the prediction of the light-front constituent-quark model (LFCQM'15) [49], the OPE reconstruction from local second moment calculations (RQCD'19) [11], the lattice calculation from LPC (LPC'22) [23], and the reconstruction from fitted moments by ANL/BNL collaboration (ANL/BNL'22) [45]. Our final result suggests the flattest and broadest distri-

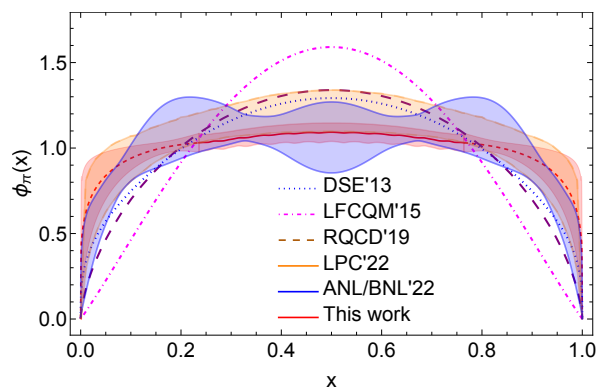


FIG. 9: Comparison of the x dependence with previous phenomenological and lattice results. In this work, the mid- x region from direct LaMET calculation is labeled with solid red line, while the endpoint regions from complementarity are labeled with dashed red lines.

bution among all these calculations, as we can also tell from the large second moment in our data. This may have a big impact on the phenomenology of pion hard exclusive processes. At large Q^2 , the $\pi\gamma\gamma^*$ transition form factor $F_{\pi\gamma\gamma}(Q^2, 0)$ [3–5, 50] and the pion electromagnetic form factor $F_\pi(Q^2)$ [51] are both sensitive to the shape of the DA $\phi(x, Q^2)$. In general, since both are enhanced near the threshold $x \rightarrow 1$ [52, 53], a broader DA will predict the form factors to be larger at large Q^2 . However, the factorization of the exclusive processes are known to be problematic near the threshold [40, 54, 55], and the scale setting in the pion electromagnetic form factor $F_\pi(Q^2)$ also causes large uncertainty to its estimation from the DA [52, 56]. Due to these complications, the study of these phenomenologies are beyond the scope of this work, but a more detailed and systematic study is needed in the future to completely understand the impacts.

VI. CONCLUSION

In this paper we have computed the pion distribution amplitude with momentum fraction in the range $x \in [0, 1]$ with improved handling of three sources of systematic errors: removing the $\mathcal{O}(\Lambda_{\text{QCD}}/xP_z)$ power correction from intrinsic ambiguities, resumming the small-momentum logarithms, and constraining the distribution near the endpoints from short distance correlations. We renormalize the matrix elements in the hybrid scheme with the LRR-improved self-renormalization factors at short distance. Then an LRR-improved matching kernel is used, along with a two-scale resummation, to obtain the pion DA in the mid- x region $x \in [0.23, 0.77]$. We then model the endpoint region with a power law function, allowing a small variation, to reconstruct coordinate space correlations and fit to our data. The second Mellin moment determined from the full- x dependence was $\langle \xi^2 \rangle = 0.302(23)$ and from the renormalization-independent short-distance OPE was $\langle \xi^2 \rangle = 0.298(39)$. These two results are in good agreement and give us confidence in the determination of the endpoint region of the DA. Our final result suggests a broad distribution of the pion DA. It has potential big impacts on the form factors of the DA at large Q^2 , and will be investigated in details in the future.

Acknowledgements

We thank MILC Collaboration for sharing the lattices used to perform this study. The LQCD calculations were performed using the Chroma software suite [57]. This research used resources of the National Energy Research Scientific Computing Center, a DOE Office of Science User Facility supported by the Office of Science of the U.S. Department of Energy under Contract No. DE-AC02-05CH11231 through ERCAP; facilities of the USQCD Collaboration are funded by the Office of Science of the U.S. Department of Energy, and the Extreme Science and Engineering Discovery Environment (XSEDE), which was supported by National Science Foundation Grant No. PHY-1548562. This research is supported by the U.S. Department of Energy, Office of Science, Office of Nuclear Physics, under contract number DE-SC0020682. J.H. is partially supported by the Center for Frontier Nuclear Science at Stony Brook University. Y.S. is partially supported by the U.S. Department of Energy, Office of Science, Office of Nuclear Physics, contract no. DE-AC02-06CH11357. The work of HL is partially supported by the US National Science Foundation under grant PHY 1653405 ‘‘CAREER: Constraining Parton Distribution Functions for New-Physics Searches’’, grant PHY 2209424, and by the Research Corporation for Science Advancement through the Cottrell Scholar Award.

Appendix A: Notations

We tabulate the various symbols used throughout this paper for the convenience of the reader in Tab. I.

| Symbol | Definition |
|---|---|
| $\tilde{h}^{\text{B}}(z, P_z, a)$ | Bare qDA in coordinate space |
| $\tilde{h}^{\text{R}}(z, P_z)$ | Renormalized qDA in coordinate space |
| $\tilde{H}^{\text{R,B}}(z, P_z)$ | $e^{izP_z/2}\tilde{h}^{\text{R,B}}(z, P_z)$ |
| $\mathcal{M}(z, P_z^{(1)}, P_z^{(2)})$ | $\tilde{H}^{\text{B}}(z, P_z^{(1)})/\tilde{H}^{\text{B}}(z, P_z^{(2)})$ |
| $\tilde{\phi}(x, P_z)$ | Renormalized qDA in momentum space |
| $\phi(x, \mu)$ | Lightcone DA in momentum space |
| $\mathcal{C}(x, y, \mu, P_z)$ | Momentum space matching kernel |
| $\mathcal{Z}(\nu, z^2, \mu^2, \lambda)$ | Coordinate space matching kernel |
| $C_{nm}(z, \mu)$ | DA Wilson coefficients |

TABLE I: Notations used throughout this paper.

Appendix B: Numerical implementation of RGR

To realize the strategy discussed in the previous section, an easy way is to write all the operators in the matrix representation. Both the quasi-DA and the lightcone DA are vectors on a grid of x_i , $\phi_i = \phi(x_i)$. The matching kernel $\hat{\mathcal{C}}$ and the evolution operator \hat{V} are now matrices on a grid of x_i and x_j , $\hat{\mathcal{C}}_{ij} = \mathcal{C}(x_i, x_j)$. Thus the resummed matching in matrix representation is

$$\begin{aligned} \tilde{\phi}_i &= \left(\left(\frac{V_{ij}^L \tilde{\phi}_j}{V_{ij} \tilde{\phi}_j} \delta_{ik} + \hat{\mathcal{C}}_{ik}^L(\mu_1) \right) \exp \left[\int_{\mu}^{\mu_1} \hat{V} d \ln \mu'^2 \right] \right)_{kl} \\ &+ \left(\frac{V_{ij}^R \tilde{\phi}_j}{V_{ij} \tilde{\phi}_j} \delta_{ik} + \hat{\mathcal{C}}_{ik}^R(\mu_2) \right) \exp \left[\int_{\mu}^{\mu_2} \hat{V} d \ln \mu'^2 \right]_{kl} \phi_l(\mu) \\ &= \hat{\mathcal{C}}_{ij}^{\text{RGR}}(\mu) \phi_j(\mu), \end{aligned} \quad (\text{B1})$$

where the resummed kernel $\hat{\mathcal{C}}^{\text{RGR}}$ now is just an $n \times n$ matrix, which can be calculated row by row.

We use an approximation of $V \otimes \tilde{\phi} = V \otimes \phi + \mathcal{O}(\alpha_s)$ to construct the ratio $(V_L^{(0)} \otimes \tilde{\phi}) / (V^{(0)} \otimes \tilde{\phi})$. However, such an approximation is not applicable to all regions, because there are zero points for $V^{(0)} \otimes \tilde{\phi}$. Near this point x_0 , the higher order term $\sim \mathcal{O}(\alpha_s)$ becomes relatively too large, and the ratio also blows up. The point x_0 of course depends on the shape of the DA and quasi-DA curve. A test on several functions suggests that $x_0 \sim 0.2$ for most DA-like functions. Thus we are still able to perform the above resummation within the region $0.23 < x < 0.77$.

In principle, the formalism may also work for $x < 0.1$ and $x > 0.9$.

Another issue of constructing the matching matrix is the endpoint regions of x . When either the scale $\mu_1 = 2xP_z$ or $\mu_2 = 2(1-x)P_z$ becomes very small, $\alpha_s(\mu)$ increases to $\mathcal{O}(1)$. In this region, the perturbative expansion in $\alpha_s(\mu)$ fails, thus the matching cannot be determined through perturbative calculations. In the numerical evaluation, these rows may blow up. Since we are calculating the matching kernel in perturbation theory, the inverse matching kernel at NLO can be expressed as

$$C^{-1}(x, y, \mu, P_z) = \delta(x - y) - \mathcal{C}^{(1)}(x, y, \mu, P_z) + \mathcal{O}(\alpha_s^2). \quad (\text{B2})$$

Applying to our matrix form, we get the inverse matching matrix

$$\hat{\mathcal{C}}_{ij}^{\text{RGR}, -1} = 2\delta_{ij} - \hat{\mathcal{C}}_{ij}^{\text{RGR}}, \quad (\text{B3})$$

which does not need the full information of the matrix to obtain a part of its inverse. So the endpoint region is no longer a problem for us to extract the resummed DA $\phi(x, \mu = 2 \text{ GeV})$ in the intermediate x region. Those endpoint regions are thus left undetermined by perturbative calculations, and may be obtained from some non-perturbative approaches in the future.

With this approach, we are able to extract the lightcone DA in the intermediate region $0.23 < x < 0.77$.

Appendix C: Perturbative matching with LRR

The LRR in the large- β_0 limit modifies the $P_z = 0$ matrix element for the DA, i.e., the Wilson coefficient $C_{00}(z, \mu)$, in the following way:

$$\begin{aligned} C_{00}^{\text{LRR}}(z, \mu, \tau) &= C_{00}^{\text{tp}}(z, \mu)|_{\text{PV}} \\ &+ \sum_i \left(C_{00}^{(i)}(z, \mu) - C_{00}^{\text{tp}, (i)}(z, \mu) \right), \end{aligned} \quad (\text{C1})$$

where $C_{00}^{\text{tp}}(z, \mu)|_{\text{PV}}$ is the leading renormalon resummed diagrams with the principal value prescription for the poles defined as scheme τ ,

$$\begin{aligned} C_{00}^{\text{tp}}(z, \mu)|_{\text{PV}} &= \int_{0, \text{PV}}^{\infty} dw e^{-4\pi w / \alpha(\mu)\beta_0} \frac{2C_F}{\beta_0} \\ &\times \left(\frac{\Gamma(1-w)e^{\frac{5}{3}w}(z^2\mu^2/4)^w}{(1-2w)\Gamma(1+w)} - 1 \right) / w, \end{aligned} \quad (\text{C2})$$

and $C_{00}^{\text{tp}, (i)}(z, \mu)$ is its expansion to a specific order. At NLO, we have

$$C_{00}^{(1)}(z, \mu) = \frac{\alpha_s C_F}{2\pi} \left(\frac{3}{2} \ln(z^2\mu^2 e^{2\gamma_E}/4) + \frac{7}{2} \right), \quad (\text{C3})$$

$$C_{00}^{\text{tp}, (1)}(z, \mu) = \frac{\alpha_s C_F}{2\pi} \left(\ln(z^2\mu^2 e^{2\gamma_E}/4) + \frac{11}{3} \right). \quad (\text{C4})$$

The LRR modifies the $P_z > 0$ matrix element $\tilde{H}(z, P_z, \mu)$ in a similar way, where the momentum dependence only enters through a phase factor,

$$\begin{aligned} \tilde{H}^{\text{LRR}}(z, P_z, \mu, \tau) &= e^{-iyzP_z} C_{00}^{\text{tp}}(z, \mu)|_{\text{PV}} \quad (\text{C5}) \\ &+ \sum_i \left(\tilde{H}^{(i)}(z, P_z, \mu) - e^{-iyzP_z} C_{00}^{\text{tp},(i)}(z, \mu) \right), \end{aligned}$$

which can be Fourier transformed to obtain the correction to the NLO matching kernel in $\overline{\text{MS}}$,

$$\begin{aligned} \Delta C^{\overline{\text{MS}}}(x, y, P_z, \mu, \tau) & \quad (\text{C6}) \\ &= \int \frac{P_z dz}{2\pi} e^{i(x-y)zP_z} \left(C_{00}^{\text{tp}}(z, \mu)|_{\text{PV}} - C_{00}^{\text{tp},(1)}(z, \mu) \right) \\ &= \int \frac{P_z dz}{2\pi} e^{i(x-y)zP_z} C_{00}^{\text{tp}}(z, \mu)|_{\text{PV}} - \frac{\alpha_s C_F}{2\pi} \frac{1}{|x-y|}, \end{aligned}$$

where the first part is not a traditional convergent function, but a distribution operating on some object through a convolution (in our case, the DA), whose effect is convergent mathematically. In practice, it is enough to perform a truncated numerical evaluation to some large z_{max} , e.g., $z_{\text{max}} = 10$ fm.

In the ratio scheme [36–38], the ratio between two momentums is free of linear divergence, thus no LRR modification is needed, and the matching kernel C^{ratio} is unchanged. In the hybrid scheme, the correction is based on the ratio scheme matching C^{ratio} , with an integration range starting from z_s during the Fourier transformation,

$$\begin{aligned} \Delta C^{\text{hybrid}}(x, y, P_z, \mu, \tau) & \\ &= 2 \int_{z_s}^{\infty} \frac{P_z dz}{2\pi} \cos((x-y)zP_z) \left(C_{00}^{\text{tp}}(z, \mu)|_{\text{PV}} - C_{00}^{\text{tp},(1)}(z, \mu) - C_{00}^{\text{tp}}(z_s, \mu)|_{\text{PV}} + C_{00}^{\text{tp},(1)}(z_s, \mu) \right) \\ &= 2 \int_{z_s}^{z_{\text{max}}} \frac{P_z dz}{2\pi} \cos((x-y)zP_z) \left(C_{00}^{\text{tp}}(z, \mu)|_{\text{PV}} - C_{00}^{\text{tp}}(z_s, \mu)|_{\text{PV}} \right) + \frac{\alpha_s C_F}{2\pi} \left(\frac{1}{|x-y|} - 2 \frac{\text{Si}((x-y)z_s P_z)}{\pi(x-y)} \right), \quad (\text{C7}) \end{aligned}$$

where the first term is calculated numerically to z_{max} in practice.

It is also easy to derive from Eq. (C5) that the LRR modification to the DA Wilson coefficient as:

$$\Delta C_{mn}^{\text{LRR}} = \delta_{mn} \left(C_{00}^{\text{tp}}(z, \mu)|_{\text{PV}} - \sum_i C_{00}^{\text{tp},(i)}(z, \mu) \right), \quad (\text{C8})$$

which can be applied to the OPE of short distance correlations.

-
- [1] M. Beneke, G. Buchalla, M. Neubert, and C. T. Sachrajda, Phys. Rev. Lett. **83**, 1914 (1999), hep-ph/9905312.
- [2] M. Beneke, G. Buchalla, M. Neubert, and C. T. Sachrajda, Nucl. Phys. B **606**, 245 (2001), hep-ph/0104110.
- [3] J. Gronberg et al. (CLEO), Phys. Rev. D **57**, 33 (1998), hep-ex/9707031.
- [4] H. J. Behrend et al. (CELLO), Z. Phys. C **49**, 401 (1991).
- [5] B. Aubert et al. (BaBar), Phys. Rev. D **80**, 052002 (2009), 0905.4778.
- [6] W. Altmannshofer et al. (Belle-II), PTEP **2019**, 123C01 (2019), [Erratum: PTEP 2020, 029201 (2020)], 1808.10567.
- [7] L. Del Debbio, M. Di Pierro, and A. Dougall, Nucl. Phys. B Proc. Suppl. **119**, 416 (2003), hep-lat/0211037.
- [8] V. M. Braun et al., Phys. Rev. D **74**, 074501 (2006), hep-lat/0606012.
- [9] R. Arthur, P. A. Boyle, D. Brommel, M. A. Donnellan, J. M. Flynn, A. Juttner, T. D. Rae, and C. T. C. Sachrajda, Phys. Rev. D **83**, 074505 (2011), 1011.5906.
- [10] G. S. Bali, V. M. Braun, M. Göckeler, M. Gruber, F. Hutzler, P. Korcyl, B. Lang, and A. Schäfer (RQCD), Phys. Lett. B **774**, 91 (2017), 1705.10236.
- [11] G. S. Bali, V. M. Braun, S. Bürger, M. Göckeler, M. Gruber, F. Hutzler, P. Korcyl, A. Schäfer, A. Sternbeck, and P. Wein (RQCD), JHEP **08**, 065 (2019), [Addendum: JHEP 11, 037 (2020)], 1903.08038.
- [12] V. Braun and D. Müller, Eur. Phys. J. C **55**, 349 (2008), 0709.1348.
- [13] V. M. Braun, S. Collins, M. Göckeler, P. Pérez-Rubio, A. Schäfer, R. W. Schiel, and A. Sternbeck, Phys. Rev. D **92**, 014504 (2015), 1503.03656.
- [14] G. S. Bali, V. M. Braun, B. Gläfle, M. Göckeler, M. Gruber, F. Hutzler, P. Korcyl, A. Schäfer, P. Wein, and J.-H. Zhang, Phys. Rev. D **98**, 094507 (2018), 1807.06671.

- [15] W. Detmold, A. Grebe, I. Kanamori, C. J. D. Lin, S. Mondal, R. Perry, and Y. Zhao (2021), 2109.15241.
- [16] X. Ji, Phys. Rev. Lett. **110**, 262002 (2013), 1305.1539.
- [17] X. Ji, Sci. China Phys. Mech. Astron. **57**, 1407 (2014), 1404.6680.
- [18] X. Ji, Y.-S. Liu, Y. Liu, J.-H. Zhang, and Y. Zhao, Rev. Mod. Phys. **93**, 035005 (2021), 2004.03543.
- [19] J.-H. Zhang, J.-W. Chen, X. Ji, L. Jin, and H.-W. Lin, Phys. Rev. D **95**, 094514 (2017), 1702.00008.
- [20] J.-H. Zhang, L. Jin, H.-W. Lin, A. Schäfer, P. Sun, Y.-B. Yang, R. Zhang, Y. Zhao, and J.-W. Chen (LP3), Nucl. Phys. B **939**, 429 (2019), 1712.10025.
- [21] R. Zhang, C. Honkala, H.-W. Lin, and J.-W. Chen, Phys. Rev. D **102**, 094519 (2020), 2005.13955.
- [22] J. Hua, M.-H. Chu, P. Sun, W. Wang, J. Xu, Y.-B. Yang, J.-H. Zhang, and Q.-A. Zhang (Lattice Parton), Phys. Rev. Lett. **127**, 062002 (2021), 2011.09788.
- [23] J. Hua et al. (Lattice Parton), Phys. Rev. Lett. **129**, 132001 (2022), 2201.09173.
- [24] X. Ji, J.-H. Zhang, and Y. Zhao, Phys. Rev. Lett. **120**, 112001 (2018), 1706.08962.
- [25] T. Ishikawa, Y.-Q. Ma, J.-W. Qiu, and S. Yoshida, Phys. Rev. D **96**, 094019 (2017), 1707.03107.
- [26] J.-W. Chen, X. Ji, and J.-H. Zhang, Nucl. Phys. B **915**, 1 (2017), 1609.08102.
- [27] X. Ji, Y. Liu, A. Schäfer, W. Wang, Y.-B. Yang, J.-H. Zhang, and Y. Zhao, Nucl. Phys. B **964**, 115311 (2021), 2008.03886.
- [28] Y.-K. Huo et al. (Lattice Parton Collaboration (LPC)), Nucl. Phys. B **969**, 115443 (2021), 2103.02965.
- [29] R. Zhang, J. Holligan, X. Ji, and Y. Su (2022), *In preparation*.
- [30] Y. Su, J. Holligan, X. Ji, F. Yao, J.-H. Zhang, and R. Zhang (2022), 2209.01236.
- [31] X. Ji (2022), 2209.09332.
- [32] I. W. Stewart and Y. Zhao, Phys. Rev. D **97**, 054512 (2018), 1709.04933.
- [33] M. Beneke, Phys. Rept. **317**, 1 (1999), hep-ph/9807443.
- [34] G. S. Bali, C. Bauer, A. Pineda, and C. Torrero, Phys. Rev. D **87**, 094517 (2013), 1303.3279.
- [35] V. M. Braun, A. Vladimirov, and J.-H. Zhang, Phys. Rev. D **99**, 014013 (2019), 1810.00048.
- [36] A. V. Radyushkin, Phys. Rev. D **96**, 034025 (2017), 1705.01488.
- [37] K. Orginos, A. Radyushkin, J. Karpie, and S. Zafeiropoulos, Phys. Rev. D **96**, 094503 (2017), 1706.05373.
- [38] A. V. Radyushkin, Phys. Lett. B **781**, 433 (2018), 1710.08813.
- [39] A. V. Efremov and A. V. Radyushkin, Theor. Math. Phys. **42**, 97 (1980).
- [40] A. V. Efremov and A. V. Radyushkin, Phys. Lett. B **94**, 245 (1980).
- [41] G. P. Lepage and S. J. Brodsky, Phys. Lett. B **87**, 359 (1979).
- [42] G. P. Lepage and S. J. Brodsky, Phys. Rev. D **22**, 2157 (1980).
- [43] T. Izubuchi, X. Ji, L. Jin, I. W. Stewart, and Y. Zhao, Phys. Rev. D **98**, 056004 (2018), 1801.03917.
- [44] Y.-S. Liu, W. Wang, J. Xu, Q.-A. Zhang, S. Zhao, and Y. Zhao, Phys. Rev. D **99**, 094036 (2019), 1810.10879.
- [45] X. Gao, A. D. Hanlon, N. Karthik, S. Mukherjee, P. Petreczky, P. Scior, S. Syritsyn, and Y. Zhao, Phys. Rev. D **106**, 074505 (2022), 2206.04084.
- [46] A. Bazavov et al. (MILC), Phys. Rev. D **87**, 054505 (2013), 1212.4768.
- [47] K. Zhang, Y.-Y. Li, Y.-K. Huo, A. Schäfer, P. Sun, and Y.-B. Yang (χ QCD), Phys. Rev. D **104**, 074501 (2021), 2012.05448.
- [48] L. Chang, I. C. Cloet, J. J. Cobos-Martinez, C. D. Roberts, S. M. Schmidt, and P. C. Tandy, Phys. Rev. Lett. **110**, 132001 (2013), 1301.0324.
- [49] J. P. B. C. de Melo, I. Ahmed, and K. Tsushima, AIP Conf. Proc. **1735**, 080012 (2016), 1512.07260.
- [50] S. Uehara et al. (Belle), Phys. Rev. D **86**, 092007 (2012), 1205.3249.
- [51] G. M. Huber et al. (Jefferson Lab), Phys. Rev. C **78**, 045203 (2008), 0809.3052.
- [52] B. Melic, B. Nizic, and K. Passek, Phys. Rev. D **60**, 074004 (1999), hep-ph/9802204.
- [53] J. Gao, T. Huber, Y. Ji, and Y.-M. Wang (2021), 2106.01390.
- [54] N. Isgur and C. H. Llewellyn Smith, Nucl. Phys. B **317**, 526 (1989).
- [55] H.-n. Li and G. F. Sterman, Nucl. Phys. B **381**, 129 (1992).
- [56] S. J. Brodsky, G. P. Lepage, and P. B. Mackenzie, Phys. Rev. D **28**, 228 (1983).
- [57] R. G. Edwards and B. Joo (SciDAC, LHPC, UKQCD), Nucl. Phys. Proc. Suppl. **140**, 832 (2005), [832(2004)], hep-lat/0409003.